

## **Mechanistic Insights into Refinery Sulfidation Corrosion**

Ishan Patel

Institute for Corrosion & Multiphase Technology  
Ohio University  
342 W. State St.  
Athens, OH 45701  
USA

Gheorghe Bota

Institute for Corrosion & Multiphase Technology  
Ohio University  
342 W. State St.  
Athens, OH 45701  
USA

David Young

Institute for Corrosion & Multiphase Technology  
Ohio University  
342 W. State St.  
Athens, OH 45701  
USA

### **ABSTRACT**

Multiple mass transport and reaction type rate processes are involved in high temperature refinery sulfidation corrosion. Corrosion tests provide only aggregate rates of corrosion which results from underlying generally sequential sub-processes. Theoretically, rates of these sub-processes can be calculated using principles of nonequilibrium thermodynamics and kinetics, if associated phenomenological coefficients are known. These coefficients are traditionally obtained by experimentally confirming the governing rate determining step. In complex systems such as refinery sulfidation corrosion, conventional empirical models such as Arrhenius, parabolic, logarithmic, or other popular rate laws cannot be confirmed exclusively. This has been elucidated by high temperature sulfidation tests manipulating concentration, temperature, and duration. Theories of solid-state chemistry and general chemical science are discussed considering the experimental data in order to create a mechanistic model which can simulate trends in corrosion rates.

Key words: corrosion mechanism, high temperature oxidation, hydrogen sulfide, sulfur, reactions (chemical)

### **INTRODUCTION**

High temperature sulfidation (or sulfidic) corrosion of steel by sulfur species in crude oil has long been known to damage refinery equipment.<sup>1</sup> Corrosion engineers have been using prediction curves derived from field corrosion data<sup>2,3</sup> to estimate rates of sulfidation corrosion. However, a significant inaccuracy is often encountered in these estimations because of the extensive diversity in molecular structures of sulfur

compounds in crude oils. Additionally, the presence of naphthenic acids complicates the problem further by influencing, physically and chemically, the sulfidation mechanism.<sup>4</sup> Hence, a reliable prediction model of sulfidation is sought after, especially in the presence of naphthenic acids.

Several models for refinery sulfidation corrosion have been published.<sup>5-11</sup> Some of these models are based on empirical laws and the rest have arbitrary relationships and “fudge factors”. An effective prediction model should secure sulfidation rate as a function of system variables such as composition of sulfur compounds, temperature, and pressure, based on a mechanistic description. In general, any specific sub-process or a step of the mechanism is validated by experimentally confirming the rate law associated with the step which relates corrosion rate with one or more system variables. Further manipulation of system variables is sought to confirm the rest of the steps. The methodology is illustrated schematically in Figure 1. When the manipulation range is limited by practicality, the remaining steps must be deduced pragmatically in the absence of other adequate methods. If none of the reaction rate laws can be distinctly identified then the reaction can be considered in “mixed control” of several mechanistic steps, meaning that the unit rates of individual steps are not significantly different. Here, the refinery sulfidation corrosion is analyzed as a mixed controlled reaction to develop useful insights into the mechanism.

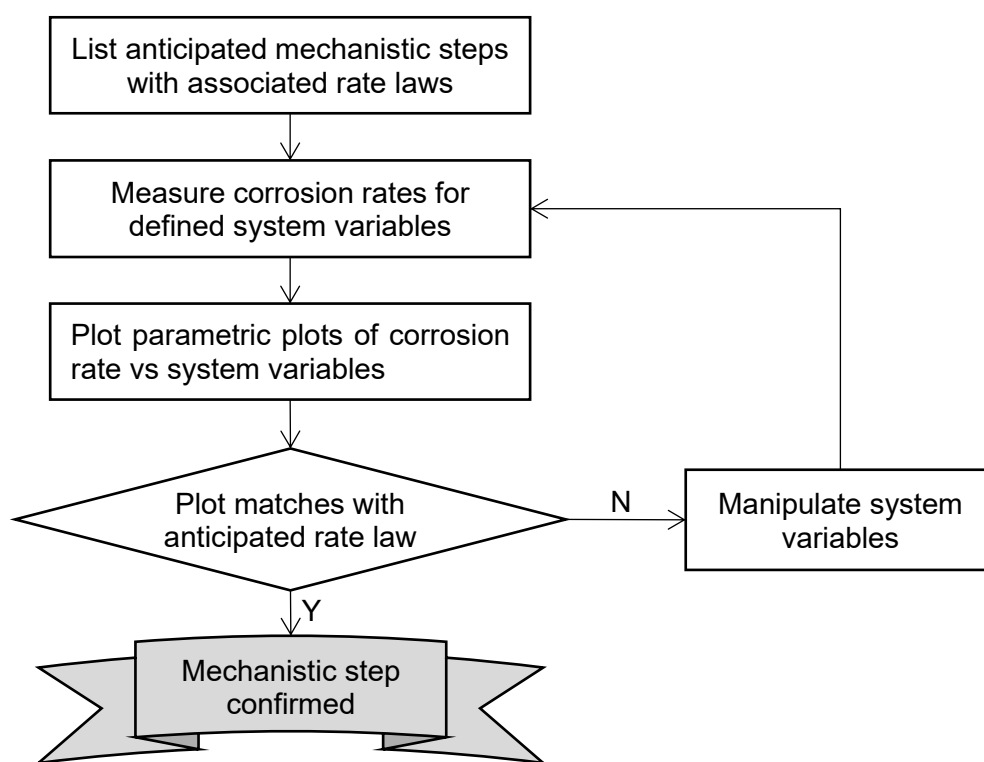


**Figure 1: Identification of a specific mechanistic step of an overall corrosion mechanism**

### Refinery Sulfidation Corrosion

An enormous variety of molecular structures of sulfur species<sup>12,13</sup> in crude oil react with steel to produce a solid corrosion product of iron sulfide scale. The overall sulfidation reaction can be described in a simplified form as follows.<sup>5,14,15</sup>



Where, R = organic moiety or hydrogen

A non-stoichiometric formula of  $\text{Fe}_{1-x}\text{S}$  for iron sulfide, also known as pyrrhotite, is used to express missing iron from the cation sites of a crystalline iron sulfide phase, resulting in vacancies.<sup>16</sup> Sulfidation

corrosion has been claimed to initially follow a parabolic type of relation between mass gain or loss vs. time and later linearize.<sup>5,6,8,17</sup> A parabolic rate law can be obtained mathematically by integration of thickness growth rate of the scale, inversely proportional to the thickness itself.<sup>18</sup> In that sense, any “scale-through” diffusion mechanism, whether molecular diffusion of corrosive species towards the metal surface or a solid-state atomic diffusion of iron and sulfur, could confirm a parabolic law.<sup>19-24</sup> However, a mechanism of molecular diffusion of corrosive species through the scale followed by their reaction with the fresh metal surface cannot be responsible for the growth of iron sulfide. This is because generated porous scale morphologies imply that iron sulfide formed in a dendritic manner in the first place by ionic transport through iron sulfide crystals.<sup>25</sup>

It can be agreed that the high temperature sulfidation of metals proceeds by ionic transport of metal and oxidant through the scale, in which interfacial oxidation of metal at the metal-sulfide interface and reduction of sulfur at the sulfide-oil interface must be warranted. Reduction of sulfur produces cationic vacancies and holes that initiate at the surface of the iron sulfide scale, and inwardly transport through the scale and get annihilated at the iron-iron sulfide interface as shown in Figure 2.<sup>16,19,26,27</sup> Hence, iron sulfide scale acts simultaneously as both an “ionic” and “electrical” conductor, this can be termed a “mixed conductor”.<sup>19,26,28</sup> If interfacial oxidation and reduction reactions are in dynamic equilibria, electrochemical potentials of ions are fixed at the interfaces establishing a potential gradient across the scale and the rate equation, derived from principles of nonequilibrium thermodynamics, approaches a parabolic law.<sup>19</sup> Local equilibria at interfaces is the main assumption behind this derivation which is valid for “thick film” regimes.<sup>19,29</sup>

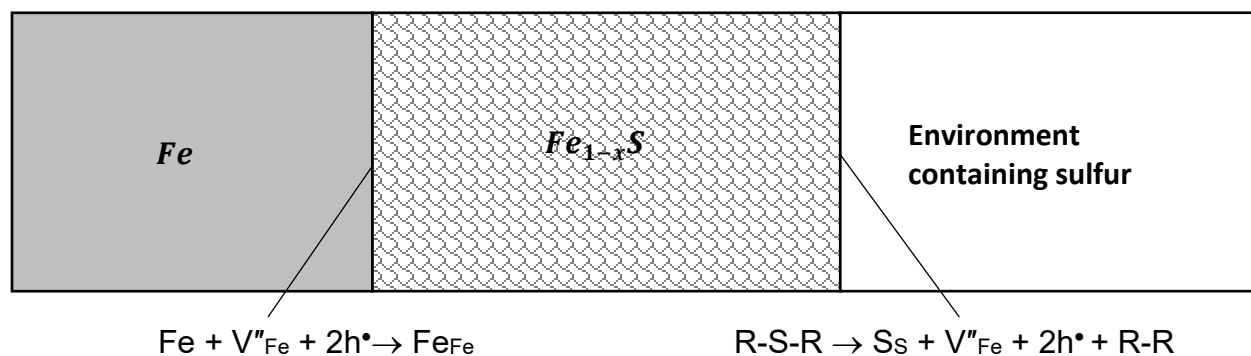


**Figure 2: Schematic representation of interfacial reactions in sulfidation corrosion using Kröger-Vink notations<sup>30,31</sup> [in  $A_S^C$ , A is a structural element (Fe, S or V=vacancy), C is a charge ( $\bullet$  = positive and ' = negative), h is a hole, and subscript S is a lattice site (Fe, S or i=interstitial)].<sup>†</sup>**

Non-stoichiometric iron sulfide  $Fe_{1-x}S$  (pyrrhotite) generally has high electrical conductivity (0.001-0.005  $\Omega$ -cm)<sup>16,32,33</sup> and the self-diffusion coefficient of iron in pyrrhotite is also relatively high,<sup>28,34</sup> which means chemical diffusivity of iron for sulfidation corrosion can be quite high for given concentration of vacancies.<sup>28</sup> In such a case, a parabolic region could get highly flattened or simply does not become rate limiting. A parabolic trend is expected only for extremely high reactivity of a sulfur compound that can greatly exceed chemical diffusion rate. In such cases, extremely high corrosion rates would result despite of diffusion control, due to high chemical diffusivity of iron in pyrrhotite.

However, in refinery sulfidation, mass loss deviates from initial “non-linear” trend and after some hours it becomes linear with time. This shifting of kinetics has been popularly referred to as “para-linear” kinetics. This kind of behavior can be modelled by adding in parallel a linearly progressing process. One such

<sup>†</sup> The term “Ionic transport” is generally used to describe atomic diffusion in crystals such as pyrrhotite due to its ionic nature.<sup>16</sup> However, theoretical treatments on the subject describe atomic diffusion by vacancy transport as opposed to ionic transport. Further, relative charges or oxidation states are more appropriately assigned to vacancies instead of elements for non-stoichiometric crystals.<sup>30</sup> Electronic transport is described using holes instead of electrons because pyrrhotite is a p-type semiconductor.<sup>16</sup>

phenomenon is oxidation with vaporization or loss of oxide scale.<sup>36</sup> Parallels can also be drawn with refinery sulfidation corrosion in which iron sulfide scale is suspected to be removed continuously. Another point of view on para-linear kinetics was postulated by Haycock involving a mechanism of continuous loss of adherent scale by recrystallization and subsequent disbonding.<sup>21,22</sup> Remaining adherent scale would thus maintain some constant thickness to yield linear kinetics.<sup>21,22</sup> The assumption is that the disbonded portion would provide no resistance to molecular diffusion of corrosive species which is incomprehensible.<sup>21,22</sup> However, a simpler explanation would be that the interfacial reactions are rate governing when the linear kinetics prevail, *i.e.*, when the mass loss is linearly proportional with time.<sup>37</sup>

Evaluation of the effect of temperature on reaction rate can also offer insights into kinetics. For most chemical reactions, an Arrhenius plot of logarithmic unit rate *versus* the inverse of absolute temperature is linear, which is expected according to transition state theory.<sup>38</sup> However, it can be hypothesized that the interfacial reactions involve complex electron transfer processes which may produce non-linearity in Arrhenius plots.<sup>39</sup> Such non-linear trends have already been observed in other sulfidation studies at refinery conditions though claimed to be linear.<sup>8,35</sup> In those studies, initial mass loss *versus* time regions were interpreted to be parabolic, an obvious outlook would be that the parabolic constant produces linear Arrhenius plots unless they did not.<sup>8,35</sup> This argument is further strengthened by the results of the present parametric study of kinetics of sulfidation reaction to determine the mechanistic steps.

## EXPERIMENTAL PROCEDURE

Traditionally, sulfidation corrosion tests have been performed in static autoclaves. In an autoclave test, the concentration of corrosive species in the test liquid decreases due to their consumption in corrosion reactions and due to their partitioning into the gas phase in the headspace. This limitation was overcome by selecting a flow-through mini autoclave (FTMA) as an experimental apparatus which is schematically shown in Figure 3. A negligible concentration gradient exists along the fluid pass over the surface of corrosion test samples, because the sulfidation rate is incredibly slow compared to the convective mass transport of species and the corrosion test samples are small, too. Also, during the test, corrosive species do not partition in the vapor phase since the liquid phase is maintained in the FTMA reactor by the back pressure valve.

The main goal of the experimental work was to determine the mechanistic steps of the sulfidation reaction, especially the rate determining step in the typical operating range of the system variables. Thus, a parametric study was performed where the system variables such as time, concentration and temperature, respectively, were manipulated. Corrosion rates were determined by mass loss from carbon steel samples within test duration instead of evaluating the mass gains (scale). In this way, the errors associated with undesirable scale loss during sample handling after testing were eliminated. After each test, the corrosion product was removed from the samples according to ASTM G1-03 procedure. Initial and final mass of samples were measured using an analytical balance. Each test had four corrosion samples in the reactor. Two were used for corrosion rate evaluation and the other two were subject to analysis of corrosion product by scanning electron microscopy (SEM) and energy dispersive X-ray spectroscopy (EDS).

---

‡ Parabolic rate constant depicts chemical diffusivity of atomic species in the scale which may also potentially generate a non-linear Arrhenius plot. However, there is a body of literature available showing linear Arrhenius plot of parabolic rate constant *versus* inverse of absolute temperature for many high temperature corrosion systems which probably drove the same conclusion of the other refinery sulfidation studies.<sup>8,35</sup>

© 2023 Association for Materials Protection and Performance (AMPP). All rights reserved. No part of this publication may be reproduced, stored in a retrieval system, or transmitted, in any form or by any means (electronic, mechanical, photocopying, recording, or otherwise) without the prior written permission of AMPP.

Positions and opinions advanced in this work are those of the author(s) and not necessarily those of AMPP. Responsibility for the content of the work lies solely with the author(s).

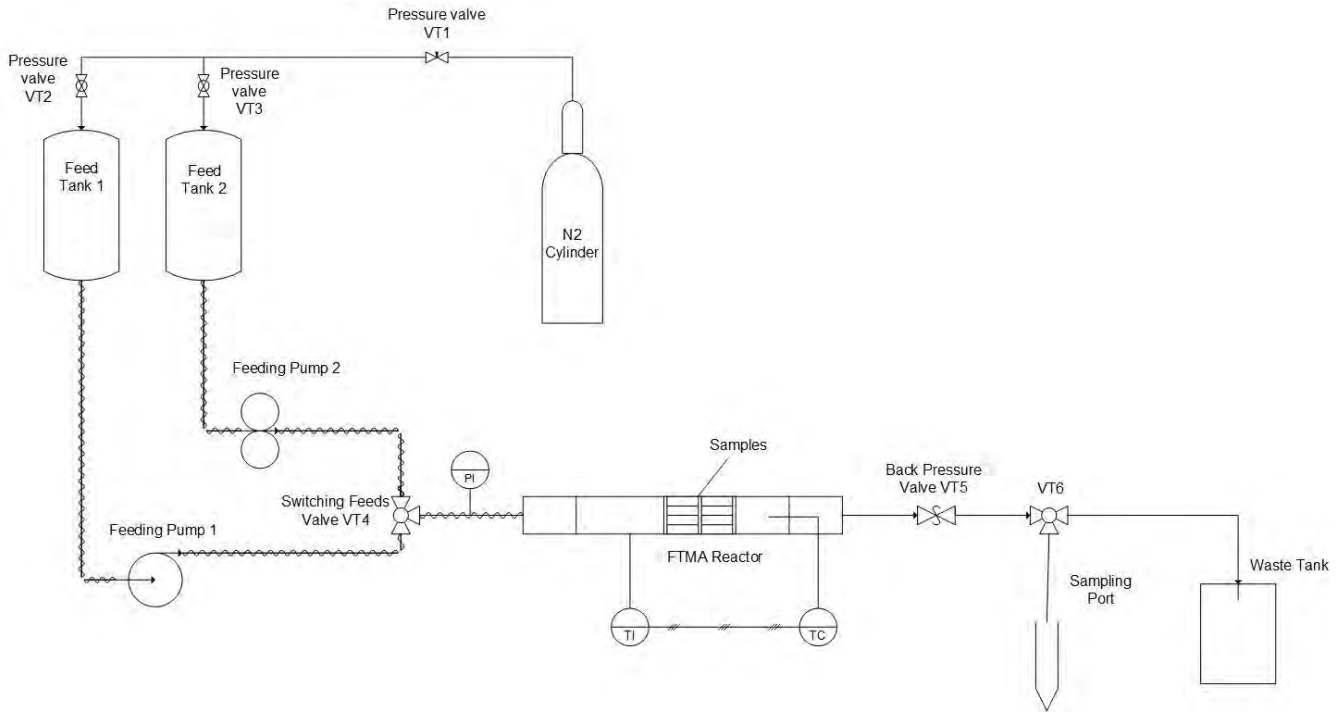


**Figure 3: Schematic diagram of testing apparatus flow-through mini autoclave (FTMA)**

Initially, it was decided to check if the sulfidation corrosion reaction was under diffusion control. A series of corrosion tests with increasing test durations up to 48 hours were performed in the flow-through-mini-autoclave (FTMA) using a model oil solution of dodecylsulfide (DDS) dissolved in a mineral oil. The increment in the test duration was chosen to be smaller (3h) for the first few tests to capture the initial rapid reaction rate, but later it was increased (6h, 12h) to obtain a notable increase in the mass loss of samples as shown in Table 1.

**Table 1 Experimental test matrix to assess evolution of sulfidation rate**

Time (h)	Total sulfur (wt.%) in test solution by DDS* in mineral oil	Test Material	Temperature (°F)	Pressure (kPa)
3	0.25	Carbon Steel (ASTM A 106)	650	600
6				
9				
12				
18				
24				
36				
48				

\*DDS = Dodecylsulfide  $\text{CH}_3(\text{CH}_2)_{11}\text{S}(\text{CH}_2)_{11}\text{CH}_3$

**Table 2 Composition of corrosion test samples of carbon steel (ASTM A 106)**

Element	C	Si	Mn	P	S	Cr	Ni	Mo	V	Cu	Fe
Wt.%	0.18	0.41	0.8	0.11	0.06	0.02	0.04	0.02	0.03	0.08	Balance

The dependence of corrosion rate on sulfur concentration was evaluated using four different concentration solutions of DDS dissolved in model oil as specified in the test matrix in Table 3.

Table 3 Experimental test matrix to assess the effect of sulfur concentration on sulfidation

Total sulfur (wt.%) in test solution by DDS in mineral oil	Test Material	Temperature (°F)	Pressure (kPa)	Time (h)
0.1	Carbon Steel	650	600	24
0.25				
0.45				
0.625				

Dependence of corrosion rate on the temperature was the most important factor from the kinetic point of view. Therefore, standard 24 hours FTMA tests were performed at 550, 600, and 650°F with a DDS solution of a constant sulfur concentration (0.45 wt.%) as given in Table 4.

Table 4 Experimental test matrix for evaluation of reaction kinetics

Temperature (°F)	Total sulfur (wt.%) in test solution by DDS in mineral oil	Test Material	Pressure (kPa)	Time (h)
550	0.45	Carbon Steel	600	24
600				
650				

## RESULTS

The aim of the experimental work was to elucidate the kinetics of sulfidation corrosion by performing parametric study of corrosion rate against time, concentrations and temperatures. Time evolution of sulfidation rates is illustrated using mass loss of corrosion test samples instead of corrosion rate because terminologies used here for evolution of the rate such as parabolic, para-linear and linear refer to evolution of mass loss *versus* time (Figure 4). Effect of concentration is illustrated using corrosion rate *versus* concentration plot (Figure 5). Effect of temperature is illustrated using Arrhenius plot of logarithmic of the unit rate *versus* inverse of the absolute temperature (Figure 6). Also, the characterization of the corrosion product was performed using scanning electron microscopy (SEM), energy dispersive X-ray spectroscopy (EDS) and X-ray diffraction (XRD).

As illustrated by Figure 4, a linear trend of mass loss *versus* time resulted from the isothermal sulfidation test with 0.25 wt.% sulfur, which supported the hypothesis that the sulfidation reaction was not under diffusion control which would have otherwise produced a parabolic trend.

Corrosion rate for 24 hours by dodecylsulfide (DDS) was linearly proportional to its concentration as illustrated by Figure 5. In contrast to the power law, which would have pointed to definitive chemical reaction control, a linear correspondence of rate with concentration could mean interfacial reaction to be rate determining. However, linear mass loss *versus* time data in Figure 4 indicates that sulfidation corrosion was in interfacial reaction control.

The Arrhenius plot of specific reaction rates *versus* inverse of the temperature was found to be non-linear as illustrated by Figure 6. This behavior was similar to the previous experiments reported for another model compound at different concentration and in different temperature ranges, which indicates that the same mechanism might be in play in all these cases.

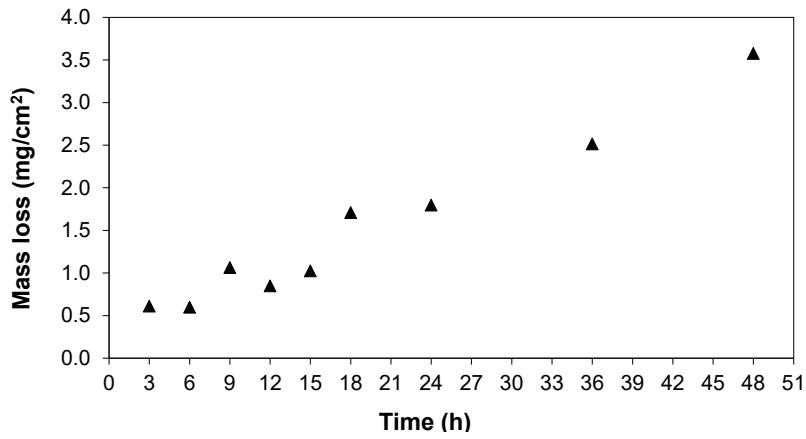


**Figure 4: Mass loss versus time data of sulfidation corrosion of carbon steel by 0.25 wt.% of sulfur by DDS in model oil solution at 650°F.**

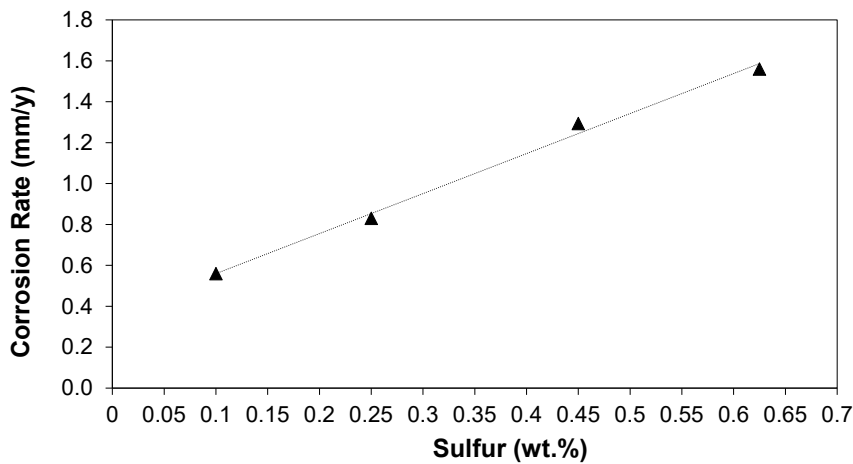


**Figure 5: Mass loss versus concentration data of sulfidation corrosion of carbon steel for 24 hours by DDS in model oil solution at 650 °F.**

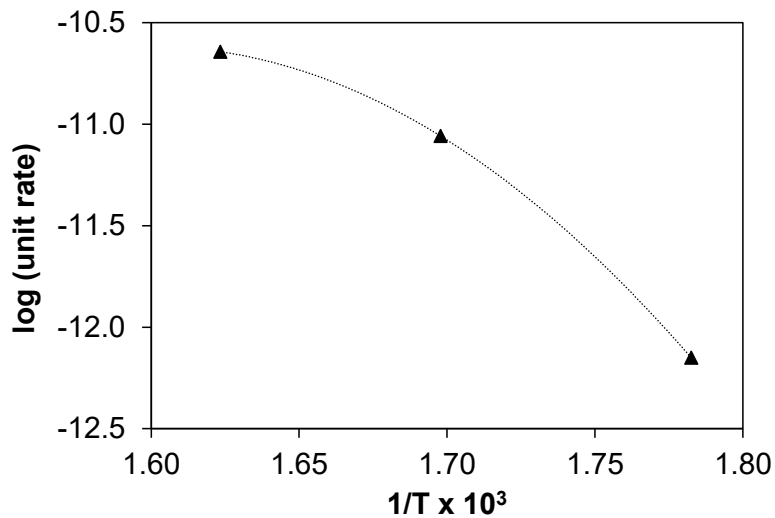


**Figure 6: Arrhenius plot of unit corrosion rate versus inverse of the absolute temperature.**

However, the comparison of the present mass loss *versus* time data with the trends reported in the other studies indicates otherwise.<sup>8,35</sup> It is possible that non-linear mass loss *versus* time trend might have been mistakenly interpreted to be parabolic instead of logarithmic in those studies.<sup>40</sup>

If a non-linear region reported in the literature<sup>8,35</sup> can be assumed to be logarithmic, then this can yield a possible explanation of the results. A logarithmic law was originally proposed by Tammann<sup>41</sup> and later derived by Cabrera and Mott based on electric field activated ionic transport through the film.<sup>42</sup> In parallel, it was proposed by Eley and Wilkinson that logarithmic kinetics could also be observed due to interfacial reactions being activated by an electric field.<sup>43</sup> The same interfacial reaction kinetics would go linear when thickness is greater than space charge region.<sup>44</sup>

As shown by Figure 7, analysis of corrosion products by scanning electron microscopy (SEM) on the surface captured the formation of new iron sulfide crystals on the outer surface which is in agreement with the hypothesis of iron sulfide growth by predominant outward diffusion of iron.

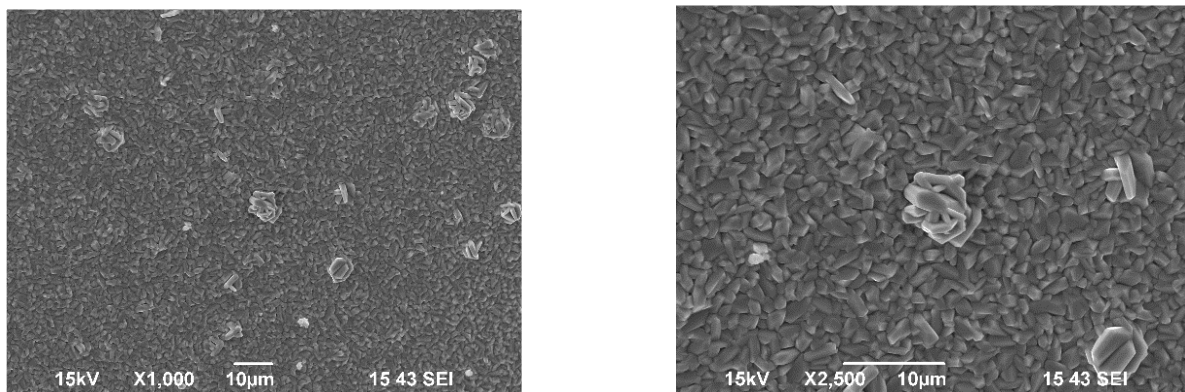


**Figure 7: Scanning electron microscopy (SEM) images of corrosion product formed on carbon steel surface by 0.25 wt.% of sulfur after 24 hours.**

Elemental analysis of corrosion product by energy dispersive X-ray spectroscopy (EDS) confirmed that corrosion product scale was composed of iron and sulfur, as illustrated by Figure 8. The corrosion product scale was disbonded from the metal surface by the epoxy embedment of the coupon allowing the resin to fill separation space. and detection of carbon and oxygen in dark regions during the EDS scanning is indicative of this, see Figure 8.

Phase identity in the scale was confirmed by sample analysis with the X-ray diffraction (XRD) at a scan rate of 3 degree/min with step width of 0.02 degree with  $\text{CuK}\alpha$  radiation generated at 30 kV and 15 mA. Peaks in the pattern were characterized to be iron and iron sulfide, as shown in Figure 9.

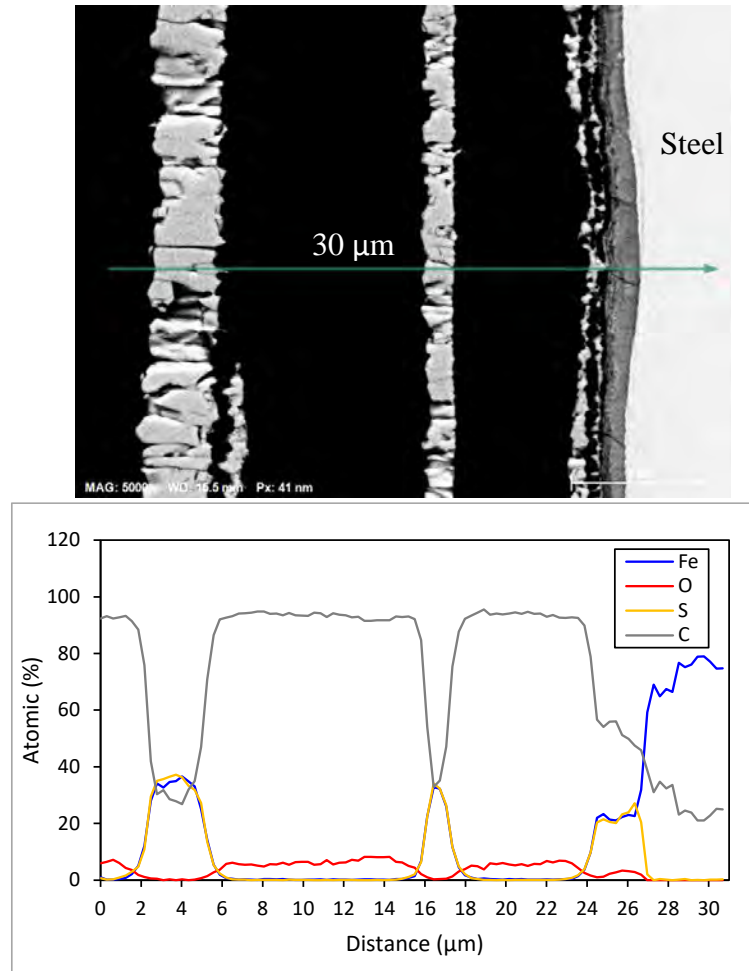


**Figure 8: Analysis of corrosion product formed on carbon steel surface by DDS (0.25 wt.% of sulfur) after 24 hours by energy dispersive X-ray spectroscopy (EDS), in scanning line mode. Black portion is epoxy.**

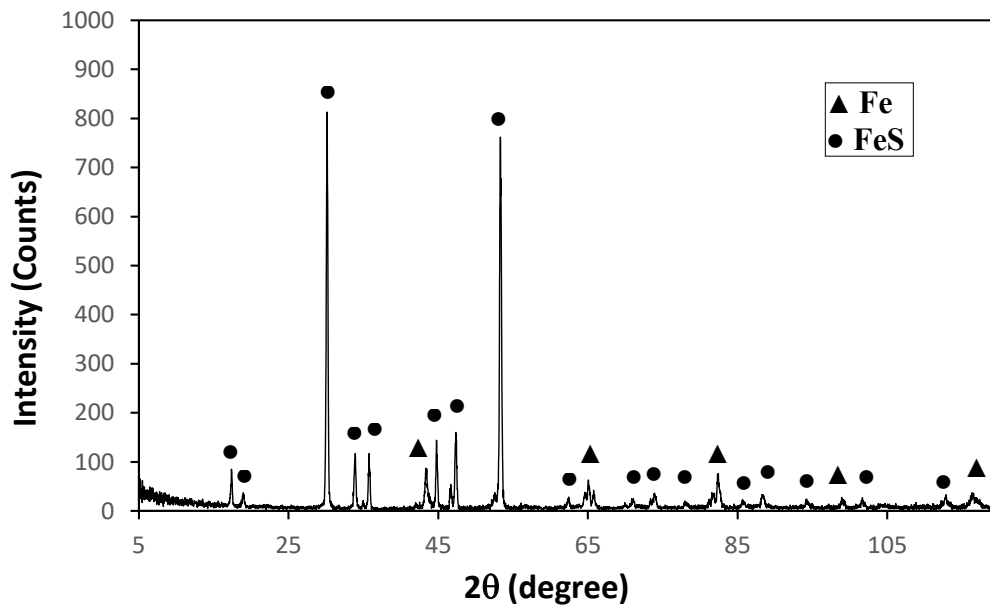


**Figure 9: X-ray diffraction pattern of corrosion test samples with corrosion product.**

## CONCLUSIONS

Refinery sulfidation corrosion proceeds by solid state diffusion of ions through the scale which is always coupled with electric current. Due to higher values of self-diffusion coefficient of iron and electrical conductivity of pyrrhotite, solid state diffusion can be much faster and may not become rate limiting which was demonstrated especially by mass loss *versus* time data. For the range of system variables selected in the experiment series, linear kinetics was observed which indicated that the rate determining step was not the solid-state diffusion but interfacial reactions. Mathematical modelling of interfacial reactions is required to be performed to estimate refinery sulfidation corrosion rates.

## ACKNOWLEDGEMENTS

The authors would like to thank the sponsors of Naphthenic Acid Corrosion Joint Industry Project (NAP JIP) at Ohio University for supporting this work and allowing to publish the experimental results.

## REFERENCES

1. R. E. Wilson, W. H. Bahlke, "Special Corrosion Problems in Oil Refining," *Ind. Eng. Chem.*, 17 (4), (1925): pp. 355–358.
2. G. Sorell, W. B. Hoyt, "Collection and Correlation of High Temperature Hydrogen Sulfide Corrosion Data—A Contribution to the Work of NACE Task Group T-5B-2 on Sulfide Corrosion at High Temperatures and Pressures in the Petroleum Industry from: The M. W. Kellogg Co., New York, N. Y.," *CORROSION*, 12 (5), (1956): pp. 33–54.
3. 34103, NACE TG 176, "Overview of Sulfidation (Sulfidic) Corrosion in Petroleum Refining Hydroprocessing Units (2014)" (NACE International Publication).
4. R. D. Kane, M. S. Cayard, "A Comprehensive Study on Naphthenic Acid Corrosion," *CORROSION*, paper no. 02555, (Denver, Colorado, NACE International, 2002), p. 16.
5. Z. A. Foroulis, "Kinetics and Mechanism of the Reaction of Iron with Sulfur Vapor in the Temperature Range of 250 to 500°C," *Mater. Corros.*, 29 (6), (1978): pp. 385–393.
6. Z. A. Foroulis, "High Temperature Degradation of Structural Materials in Environments Encountered in the Petroleum and Petrochemical Industries: Some Mechanistic Observations," *Anti-Corros. Methods Mater.*, 32 (11), (1985): pp. 4–9.
7. D. Farrell, L. Roberts, "A Study of High Temperature Sulfidation Under Actual Process Conditions," *CORROSION*, paper no. 10358 (San Antonio, Texas, NACE International, 2010), p. 11.
8. S. Sharifi-Asl, A. Liang, D. Cooke, D. R. Chapman, B. Chaloner-Gill, A. E. Kuperman, "High-Temperature Sulfidic Corrosion of Carbon Steel in Model Oil/Sulfur Compound Blends," *CORROSION*, paper no. 8909 (New Orleans, Louisiana, NACE International, 2017).
9. P. Jin, W. Robbins, G. Bota, "High-Temperature Corrosion by Carboxylic Acids and Sulfidation under Refinery Conditions—Mechanism, Model, and Simulation" *Ind. Eng. Chem. Res.*, 57 (12), (2018): pp. 4329–4339.
10. K. Toba, S. Miyamoto, S. Tokuoka, "A New Prediction Tool for Sulfidation Corrosion in Crude Units," *CORROSION*, paper no. 16762 (Virtual, NACE International, 2021).
11. A. Wing, W. Robbins, G. Buchheim, F. Sapienza, "Introducing an Innovative Simultaneous Naphthenic Acid, Sulfidation and Mass Transport Corrosion Model for Crudes and Sidestreams," *CORROSION*, paper no. 16755 (Virtual, NACE International, 2021).
12. J. M. Schmitter, P. Arpino, G. Guiochon, "Investigation of High-Molecular-Weight Carboxylic Acids in Petroleum by Different Combinations of Chromatography (Gas and Liquid) and Mass Spectrometry (Electron Impact and Chemical Ionization)," *J. Chromatogr. A*, 167, (1978): pp. 149–158.
13. T. Y. Ho, M. A. Rogers, H. V. Drushel, C. B. Koons, "Evolution of Sulfur Compounds in Crude Oils," *AAPG Bull.*, 58, (1974): pp. 2338–2348.

14. E. Babaian-Kibala, H. L. Craig Jr., G. L. Rusk, K. V. Blanchard, T. J. Rose, B. L. Uehlein, R. C. Quinter, M. A. Summers, "Naphthenic Acid Corrosion in Refinery Settings". *Mater. Perform.*, 32 (4), (1993): pp. 50–55.
15. D. J. Young, *High Temperature Oxidation and Corrosion of Metals*, 2<sup>nd</sup> ed. (Oxford, UK: Elsevier, 2016), pp. 81–137.
16. D. J. Vaughan, J. R. Craig, *Mineral Chemistry of Metal Sulfides*, 1<sup>st</sup> ed. (Cambridge, UK, New York, USA: Cambridge University Press, 1978), pp. 18–71.
17. M. El Kamel, A. Galtayries, P. Vermaut, B. Albinet, G. Foulonneau, X. Roumeau, B. Roncin, P. Marcus, "Sulfidation Kinetics of Industrial Steels in a Refinery Crude Oil at 300 °C: Reactivity at the Nanometer Scale," *Surf. Interface Anal.*, 42 (6–7), (2010): pp. 605–609.
18. G. Tammann, "Über Anlauffarben von Metallen," *Z. Für Anorg. Allg. Chem.*, 111 (1), (1920): pp. 78–89.
19. C. Wagner, "Beitrag Zur Theorie Des Anlaufvorgangs," *Z. Für Phys. Chem.*, 21B (1), (1933): pp.25–40.
20. C. Wagner, "Theoretical Analysis of the Diffusion Processes Determining the Oxidation Rate of Alloys," *J. Electrochem. Soc.*, 99 (10), (1952): pp. 369–380.
21. E. W. Haycock, "Transitions from Parabolic to Linear Kinetics in Scaling of Metals," *J. Electrochem. Soc.*, 106 (9), (1959): pp. 771–775.
22. E. W. Haycock, "High-Temperature Sulfiding of Iron Alloys in Hydrogen Sulfide-Hydrogen Mixtures," *J. Electrochem. Soc.*, 106 (9), (1959): pp. 764–771.
23. B. E. Deal, A. S. Grove, "General Relationship for the Thermal Oxidation of Silicon," *J. Appl. Phys.*, 36 (12), (1965): pp. 3770–3778.
24. D. E. Coates, A. D. Dalvi, "An Extension of the Wagner Theory of Alloy Oxidation and Sulfidation," *Oxid. Met.*, 2 (4), (1970): pp. 331–347.
25. P. Kofstad, "On the Formation of Porosity and Microchannels in Growing Scales," *Oxid. Met.*, 24 (5–6), (1985): pp. 265–276.
26. T. P. Hoar, L. E. Price, "The Electrochemical Interpretation of Wagner's Theory of Tarnishing Reactions," *Trans. Faraday Soc.*, 34, (1938): pp. 867–872.
27. K. Hauffe, L. Pethe, R. Schmidt, S. R. Morrison, "On the Mechanism of Formation of Thin Oxide Layers on Nickel," *J. Electrochem. Soc.*, 115 (5), (1968): pp. 456–461.
28. J. Maier, "Defect Chemistry: Composition, Transport, and Reactions in the Solid State; Part II: Kinetics," *Angew. Chem. Int. Ed. Engl.*, 32 (4), (1993): pp. 528–542.
29. Z. Xu, K. M. Rosso, S. Brummer, "Metal Oxidation Kinetics and the Transition from Thin to Thick Films," *Phys. Chem. Chem. Phys.*, 14 (42), (2012): pp. 14534–14539.
30. F. A. Kröger, H. J. Vink, *Relations between the Concentrations of Imperfections in Crystalline Solids*, in *Solid State Physics*, Vol. 3, (New York, USA: Academic Press, 1956); pp 307–435.
31. D. J. Young, W. W. Smeltzer, "Sulfidation Kinetics of Iron and Ferritic Iron-Cobalt Alloys," *J. Electrochem. Soc.*, 123 (2), (1976): pp. 229–234.
32. H. U. Worm, D. Clark, M. J. Dekkers, "Magnetic Susceptibility of Pyrrhotite: Grain Size, Field and Frequency Dependence," *Geophys. J. Int.*, 114 (1), (1993): pp. 127–137.
33. C. I. Pearce, "Electrical and Magnetic Properties of Sulfides," *Rev. Mineral. Geochem.*, 61 (1), (2006): pp. 127–180.
34. F. William Herbert, A. Krishnamoorthy, L. Rands, K. J. Van Vliet, B. Yildiz, "Magnetic Diffusion Anomaly at the Néel Temperature of Pyrrhotite, Fe<sub>1-x</sub>S," *Phys. Chem. Chem. Phys.*, 17 (16), (2015): pp. 11036–11041.
35. D. R. Qu, Y. G. Zheng, H. M. Jing, Z. M. Yao, W. Ke, "High Temperature Naphthenic Acid Corrosion and Sulphidic Corrosion of Q235 and 5Cr1/2Mo Steels in Synthetic Refining Media," *Corros. Sci.*, 48 (8), (2006): pp. 1960–1985.
36. C. S. Tedmon, "The Effect of Oxide Volatilization on the Oxidation Kinetics of Cr and Fe-Cr Alloys," *J. Electrochem. Soc.*, 113 (8), (1966): pp. 766–768.
37. H. Schmalzried, "Chemical Kinetics at Solid-Solid Interfaces," *Pure Appl. Chem.*, 72 (11), (2000): pp. 2137–2147.
38. H. Eyring, "The Activated Complex in Chemical Reactions," *J. Chem. Phys.* (1935), 3, pp. 107–115.

39. R. A. Marcus, "On the Theory of Electron-Transfer Reactions. VI. Unified Treatment for Homogeneous and Electrode Reactions," *J. Chem. Phys.*, 43 (2), (1965): pp. 679–701.
40. T. A. Ramanarayanan, S. N. Smith, Corrosion of Iron in Gaseous Environments and in Gas-Saturated Aqueous Environments," *CORROSION*, 46 (1), (1990): 66–74.
41. G. Tammann, W. Köster, "Metallographische Mitteilungen Aus Dem Institut Für Physikalische Chemie Der Universität Göttingen. CV. Die Geschwindigkeit Der Einwirkung von Sauerstoff, Schwefelwasserstoff Und Halogenen Auf Metalle.," *Z. Für Anorg. Allg. Chem.*, 123 (1), (1922): pp. 196–224.
42. N. Cabrera, N. F. Mott, "Theory of the Oxidation of Metals," *Rep. Prog. Phys.*, 12 (1), (1949): pp. 163–184.
43. D. D. Eley, P. R. Wilkinson, "Adsorption and Oxide Formation on Aluminium Films," *Proc. R. Soc. Lond. Ser. Math. Phys. Sci.*, 254 (1278), (1960): pp. 327–342.
44. C. Wagner, "The Formation of Thin Oxide Films on Metals," *Corros. Sci.*, 13 (1), (1973): pp. 23–52.